

Synthesis of novel narrow-band-gap copolymers based on [1,2,5]thiadiazolo[3,4-*f*]benzotriazole and their application in bulk-heterojunction photovoltaic devices

Yang Dong, Wanzhu Cai, Xiaowen Hu, Chengmei Zhong, Fei Huang*, Yong Cao

Institute of Polymer Optoelectronic Materials and Devices, State Key Laboratory of Luminescent Materials and Devices, South China University of Technology, Guangzhou 510640, PR China

ARTICLE INFO

Article history:

Received 5 December 2011
Received in revised form
5 February 2012
Accepted 7 February 2012
Available online 13 February 2012

Keywords:

[1,2,5]Thiadiazolo[3,4-*f*]benzotriazole
Alternating copolymer
Polymer solar cells

ABSTRACT

Two novel conjugated alternating copolymers with [1,2,5]thiadiazolo[3,4-*f*]benzotriazole as acceptor and 9,9-dioctylfluorene or *N*-9'-heptadecanyl-carbazole as donors respectively, were synthesized by Suzuki polycondensation. Both of the two copolymers have nearly ideal band gaps and show excellent absorption spectra in near infrared region. Polymer solar cells based on the blends of them and [6,6]-phenyl-C₇₁ butyric acid methyl ester show excellent performance when using a water/alcohol soluble conjugated polymer as cathode interlayer, which exhibit a maximum power conversion efficiency of 3.17% with the short-circuit current density of 8.50 mA/cm², the open-circuit voltage of 0.70 V and the fill factor of 41%. Our results demonstrate that [1,2,5]thiadiazolo[3,4-*f*]benzotriazole is a promising acceptor unit for low band gap polymer donor materials design.

© 2012 Elsevier Ltd. All rights reserved.

1. Introduction

In the past decade, polymer solar cells (PSCs), especially bulk-heterojunction (BHJ) PSCs, have attracted considerable attention due to their advantages over traditional silicon-based solar cells for their low cost, light weight, and the facility for solvent process [1–6]. Huge progress has been made in the past decade as the power conversion efficiencies (PCEs) of PSCs have been improved from 1% to more than 9% [7]. To achieve PSCs with high performance, the BHJ active layer materials, especially the polymer donor materials are very important. An ideal polymer donor material should have suitable low band gap and good π – π stacking to maximize sunlight absorption and consequently high short circuit current (J_{sc}), high charge carrier mobility to get high fill factor (FF). Furthermore, the highest occupied molecular orbital (HOMO) of the polymer should be low, which will enhance the resulting PSCs' open circuit voltage (V_{oc}). Lastly, the polymer should have excellent solubility for compatibility with solution process. To meet all these requirements, one common strategy of donor material design is the use of donor–acceptor (D–A) copolymer structure, in which an electron donor unit and an electron acceptor unit form an alternating copolymer to effectively lower the band gap of the resulting polymer [8]. Moreover, the energy levels and band gaps of the

designed D–A copolymers can be readily tuned by controlling the intramolecular charge transfer (ICT) from the donor units to the acceptor units. By this approach, many D–A copolymer donor materials have been developed and exhibited promising photovoltaic performances with PCEs in the range of ~3–7% [9–24].

Benzo[1,2,5]thiadiazole (BT) has been widely used as the electron acceptor unit in D–A copolymer design due to its existence of the heteroatom interactions, excellent π – π stacking, and simple synthesis [25]. However, the electron withdraw capability of BT is not strong and the band gaps of the BT-based D–A copolymers are relative large and not optimal for efficient sunlight harvesting [21,24,26]. Moreover, the solubilities of many BT based D–A copolymers are relatively poor, which limit their compatibility with solution process. Thereby, much effort has been put into modification of the BT-based acceptor units to obtain D–A conjugated materials with optimal band gaps and improved solubility for solar cell applications. Bo et al. synthesized alkoxy BT based D–A copolymers which showed better solubility and thereby improved photovoltaic performance compared to those BT-based analogous D–A polymers [27–29]. Recently, You et al. reported the D–A copolymers based on a fluorine substituted BT, which exhibited promising photovoltaic performance with PCEs exceeded 7% [30]. Besides, benzo[1,2-*c*;4,5-*c'*]bis[1,2,5]thiadiazole, [1,2,5]thiadiazolo[3,4-*g*]quinoxaline and their derivatives have also been developed which exhibited much stronger electron withdrawing capability than BT. However, the strong electron affinities of the resulting polymers affected the charge separation efficiencies

* Corresponding author.

E-mail address: msfhuang@scut.edu.cn (F. Huang).

between the polymers and [6,6]-phenyl-C₆₁ butyric acid methyl ester (PC₆₁BM) or [6,6]-phenyl-C₇₁ butyric acid methyl ester (PC₇₁BM), leading to a poor device performance despite of their dramatically lowered band gaps [31–40]. Thereby, it is critical to find a balance between the band gaps and the electron affinities of the donor materials for PSCs application.

Benzotriazole (BTA) is another promising electron-withdrawing building block [41] for PSC and polymer light emitting device (PLED) applications. Although its electron-withdrawing capability is weaker compared with BT [42–44], the BTA has a better solubility because of the modifiability of the N atom on the triazole ring, which enable the linkage long alkyl side chains for a good solubility. To take the advantages of BT and BTA units, here we use a new electron-withdrawing building block [1,2,5]thiadiazolo[3,4-*f*]benzotriazole (TZBT), which combined both the merits of BT and BTA [45], as the acceptor in D–A system. Two novel D–A copolymers: poly [2,7-(9,9-dioctylfluorenyl)-*alt*-5,5-(4',8'-di-2-thienyl)-6-(2-ethylhexyl)-[1,2,5]thiadiazolo[3,4-*f*]benzotriazole] (PF-TZBT) and poly [N-9'-heptadecanyl-2,7-carbazole-*alt*-5,5-(4',8'-di-2-thienyl)-6-(2-ethylhexyl)-[1,2,5]thiadiazolo[3,4-*f*]benzotriazole] (PCZ-TZBT) were developed. It was found that the band gaps of the resulting copolymers were effectively lowered and their solubilities were also improved due to the linked alkyl side chains on the triazole rings. The photovoltaic properties of the resulting copolymers were investigated and the PSC devices based on these polymers exhibited good performances.

2. Experimental section

2.1. Measurement and characterization

¹H and ¹³C NMR spectra were measured on Bruker DRX 300 and Varian INOVA 500NB spectrometers operating at 300 MHz and 75 MHz respectively. Chemical shifts were reported as δ value (ppm) relative to an internal tetramethylsilane (TMS) standard. The number-average molecular weights (M_n), weight-average molecular weights (M_w) and polydispersity index (PDI) were determined at 150 °C by a PL-GPC 220 type in 1,2,4-trichlorobenzene using a calibration curve with standard polystyrene as a reference. Thermogravimetric analysis (TGA) was performed on Netzsch TG 209 in nitrogen, with a heating rate of 20 °C min⁻¹. Cyclic voltammograms (CV) were recorded on a CHI 660A electrochemical workstation. The CV was performed in a solution of tetrabutylammonium hexafluorophosphate (Bu₄NPF₆) (0.1 M) in acetonitrile, using saturated calomel electrode (SCE) and a platinum wire as reference and counter electrode, respectively, at a scan rate of 50 mV/s at room temperature. A platinum electrode coated with thin copolymer film was used as the working electrode. Elemental analyses were performed on a Vario EL elemental analysis instrument (Elementar Co.).

2.2. Device fabrication and characterization

Indium tin oxide (ITO)-coated glass substrates (20–30 Ω /per square) were cleaned by de-ionized water, acetone, sonication in detergent and isopropyl alcohol, and dried in oven under 70 °C for at least 6 h. Then, treated with an oxygen plasma for 5 min, a 40 nm thick layer of poly(3,4-ethylenedioxythiophene):poly(styrenesulfonate) (PEDOT:PSS) (Baytron P VP Al 4083, filtered at 0.45 μ m) was first spin-coated on the pre-cleaned ITO-coated glass substrates at 3000 rpm and baked at 150 °C for 15 min under ambient condition. The following fabrication process was then finished in an argon-filled glove-box. Each composite was dissolved in solution separately before solution mixing to get a homogeneously blended solution. Proper spin-coating speed was chosen to

get ~75 nm thick active layer for different composite. For PF-TZBT:PC₆₁BM, the spin speed was 1600 rpm; For PCZ-TZBT:PC₆₁BM, the spin speed is 1800 rpm. Then, an ultra thin poly [(9,9-dioctyl-2,7-fluorenyl)-*alt*-(9,9-bis(30-(N,N-dimethylamino)propyl)-2,7-fluorenyl)] (PFN) film (5 nm) coated from 0.2 mg/ml methanol solution on the active layer. The substrates were pumped down to high vacuum ($<4 \times 10^{-6}$ mbar), and aluminum (100 nm) was thermally evaporated onto the active layer. The effective area (0.16 cm²) is defined by a shadow mask. The last step is encapsulating the substrates by a thin glass slice.

The current–voltage (*J*–*V*) characteristics of photovoltaic devices were measured in ambient air using a Keithley 2400 source-measurement unit. A solar simulator (Oriel model 91192) was used.

The device structure of space charge limited current (SCLC) studies is ITO/PEDOT/polymer/MoO₃ (10 nm)/Al. The mobility was determined by fitting the dark current to the model of a single carrier SCLC, which is described by the child law. The effective voltage can be obtained by subtracting the built-in voltage (V_{bi}) and the voltage drop (V_s) from the substrate's series resistance from the applied voltage (V_{appl}), $V = V_{appl} - V_{bi} - V_s$. The hole-mobility can be calculated from the slope of the $J^{1/2} \sim V$ curves. The effective area was also 0.16 cm².

The spectral response was measured with a commercial photo modulation spectroscopic setup. A calibrated Si photodiode was used to determine the photosensitivity.

2.3. Materials

All the starting materials were purchased from Aldrich or Alfa Aesar and used without further purification. All the reactions were carried out under argon at 1 atm unless mentioned otherwise. Tetrahydrofuran (THF) were distilled from sodium before use. 4,7-Dibromo-5,6-dinitro-benzo[1,2,5]thiadiazole (**2**), 5,6-dinitro-4,7-bis(thiophen-2-yl)-benzo[1,2,5]thiadiazole (**3**), 5,6-diamino-4,7-bis(thiophen-2-yl)-benzo[1,2,5]thiadiazole (**4**) [39], 2,7-bis(4',4',5',5'-tetramethyl-1',3',2'-dioxaborolan-2'-yl)-9,9-dioctylfluorene (**8**) [26] and 2,7-bis(4',4',5',5'-tetramethyl-1',3',2'-dioxaborolan-2'-yl)-N-9'-heptadecanyl-carbazole (**9**) [21] were prepared according to the published literatures.

2.3.1. Synthesis of 4,8-bis(thiophen-2-yl)-5H-[1,2,5]thiadiazolo[3,4-*f*]benzotriazole (**5**)

5,6-Diamino-4,7-bis(thiophen-2-yl)-benzo[1,2,5]thiadiazole (**4**) (2 g, 5 mmol) was added into the beaker with the solution of acetic acid (30 ml) and water (30 ml), then THF was added until the mixture was totally dissolved. The beaker was cooled to 0–5 °C using ice-bath. The solution of NaNO₂ (0.38 g, 5.5 mmol) in water was carefully added into the beaker dropwise. The resulting reaction mixture was kept stirring for 10 min, then heated to 80 °C for 1 h. After cooling to the room temperature, the mixture was poured into water and extracted with dichloromethane for three times. The solvent was removed and the crude product was dried under reduced pressure without further purification.

2.3.2. Synthesis of 4,8-bis(thiophen-2-yl)-6-(2-ethylhexyl)-[1,2,5]thiadiazolo[3,4-*f*]benzotriazole (**6**)

4,8-Bis(thiophen-2-yl)-5H-[1,2,5]thiadiazolo[3,4-*f*]benzotriazole (**5**) (3 g, 8.8 mmol) was dissolved in 50 ml distilled N,N-dimethylformamide (DMF), potassium t-butoxide (1.12 g, 10 mmol) and 2-bromoethylheptane (1.92 g, 10 mmol) was added and the mixture was stirred under reflux for 24 h. After solvent was removed by evaporation, column chromatography on silica gel was performed to yield 0.92 g (23%) **6** as dark blue solid. ¹H NMR (CDCl₃, 300 MHz) δ (ppm): 8.75 (dd, 2H), 7.58 (dd, 2H), 7.27 (m, 2H), 4.80

(dd, 2H), 2.33 (t, 1H), 1.24–1.48 (m, 8H), 0.88–1.0 (m, 6H). ^{13}C NMR (CDCl_3 , 75 MHz) δ (ppm): 149.8, 142.6, 137.2, 130.9, 129.2, 127.6, 111.9, 60.9, 40.6, 30.7, 28.5, 24.1, 22.9, 14.0, 10.6. Anal. calcd for $\text{C}_{22}\text{H}_{23}\text{N}_5\text{S}_3$ (%): C 58.25, H 5.11, N 15.44, S 21.20. Found (%): C 58.03, H 5.14, N 15.33, S 21.22.

2.3.3. Synthesis of 4,8-bis(5-bromo-thiophen-2-yl)-6-(2-ethylhexyl)-[1,2,5]thiadiazolo[3,4-f]benzotriazole (7)

4,8-Bis(thiophen-2-yl)-6-(2-ethylhexyl)-[1,2,5]thiadiazolo[3,4-f]benzotriazole (**6**) (2 g, 4.4 mmol) was dissolved in 50 ml THF and *N*-bromosuccinimide (NBS) (1.78 g, 9.68 mmol) in THF solution was added dropwise and kept stirring at room temperature overnight. After evaporating the solvent, the product was purified with column chromatography to yield 2.31 g (86%) **7** as dark blue powder. ^1H NMR (CDCl_3 , 300 MHz) δ (ppm): 7.60 (dd, 2H), 7.28 (dd, 2H), 4.80 (dd, 2H), 2.33 (t, 1H), 1.24–1.48 (m, 8H), 0.88–1.0 (m, 6H). ^{13}C NMR (CDCl_3 , 75 MHz) δ (ppm): 149.0, 141.8, 138.6, 130.9, 130.4, 117.7, 110.8, 60.9, 40.6, 30.7, 28.5, 24.1, 23.0, 14.1, 10.6. Anal. calcd for $\text{C}_{22}\text{H}_{21}\text{Br}_2\text{N}_5\text{S}_3$ (%): C 43.22, H 3.46, N 11.45, S 15.73. Found (%): C 43.03, H 3.48, N 11.20, S 15.82.

2.3.4. Synthesis of PF-TZBTIT

4,8-Bis(5-bromo-thiophen-2-yl)-6-(2-ethylhexyl)-[1,2,5]thiadiazolo[3,4-f]benzotriazole (**7**) (0.3044 g, 0.5 mmol), 2,7-bis(4',4',5',5'-tetramethyl-1',3',2'-dioxaborolan-2'-yl)-9,9-dioctylfluorene (**8**) (0.32 g, 0.5 mmol), $\text{Pd}(\text{PPh}_3)_4$ (8 mg) were dissolved in 15 ml toluene and 20% aqueous tetraethyl ammonium hydroxide (2 ml) under the protection of argon in a 50 ml two-necked round-bottomed flask. The mixture was refluxed with vigorously stirring in the dark for 5 h under an argon atmosphere. After cooling to room temperature, the mixture was poured into 300 ml methanol. The precipitated material was collected by filtration through a funnel. After washing with acetone for 24 h in a Soxhlet apparatus to remove oligomers and catalyst residues, the resulting material was dissolved in 30 ml chlorobenzene. The solution was filtered with a PTFE filter, concentrated, and

precipitated from methanol to yield PF-TZBTIT as a dark green solid (320 mg, 80%). ^1H NMR (*o*-DCB- d_4 , 300 MHz) δ (ppm): δ 9.13 (s, 2H), 8.12–7.76 (m, 8H), 4.94 (dd, 2H), 2.45–2.16 (m, 5H), 1.77–0.82 (m, 42H). GPC (1,2,4-trichlorobenzene, polystyrene standard): $M_n = 10.3$ kDa, $M_w = 29.9$ kDa, PDI = 2.90. Anal. calcd. for $\text{C}_{53}\text{H}_{67}\text{N}_5\text{S}_3$ (%): C 73.14, H 7.76, N 8.05, S 11.05. Found (%): C 72.13, H 7.35, N 8.27, S 11.85.

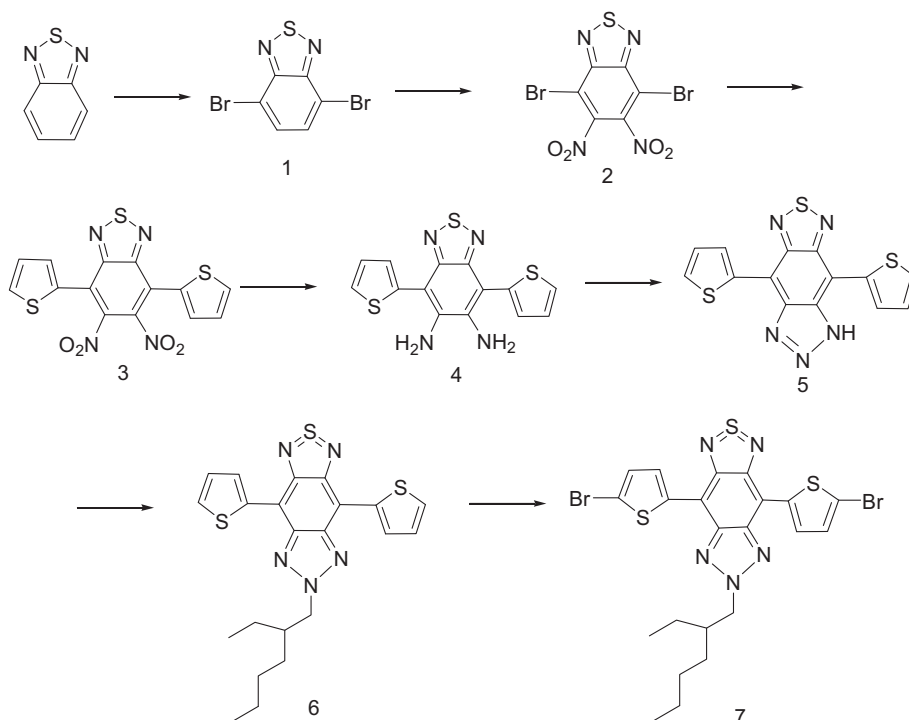
2.3.5. Synthesis of PCZ-TZBTIT

PCZ-TZBTIT was prepared according to the same procedure as that for PF-TZBTIT (150 mg, 57.5%), and 2,7-bis(4',4',5',5'-tetramethyl-1',3',2'-dioxaborolan-2'-yl)-*N*-9'-heptadecanylethylcarbazole (**9**) was used in the polymerization. ^1H NMR(*o*-DCB- d_4 , 300 MHz) δ (ppm): 8.93 (s, 2H), 8.63–7.62 (m, 8H), 5.38 (m, 2H), 4.98 (s, 1H), 2.50 (m, 4H), 2.11 (m, 4H), 1.69–0.88 (m, 40H). GPC (1,2,4-trichlorobenzene, polystyrene standard): $M_n = 12.8$ kDa, $M_w = 37.4$ kDa, PDI = 2.92. Anal. calcd for $\text{C}_{53}\text{H}_{68}\text{N}_6\text{S}_3$ (%): C 71.90, H 7.74, N 9.49, S 10.87. Found (%): C 71.23, H 7.44, N 9.89, S 11.32.

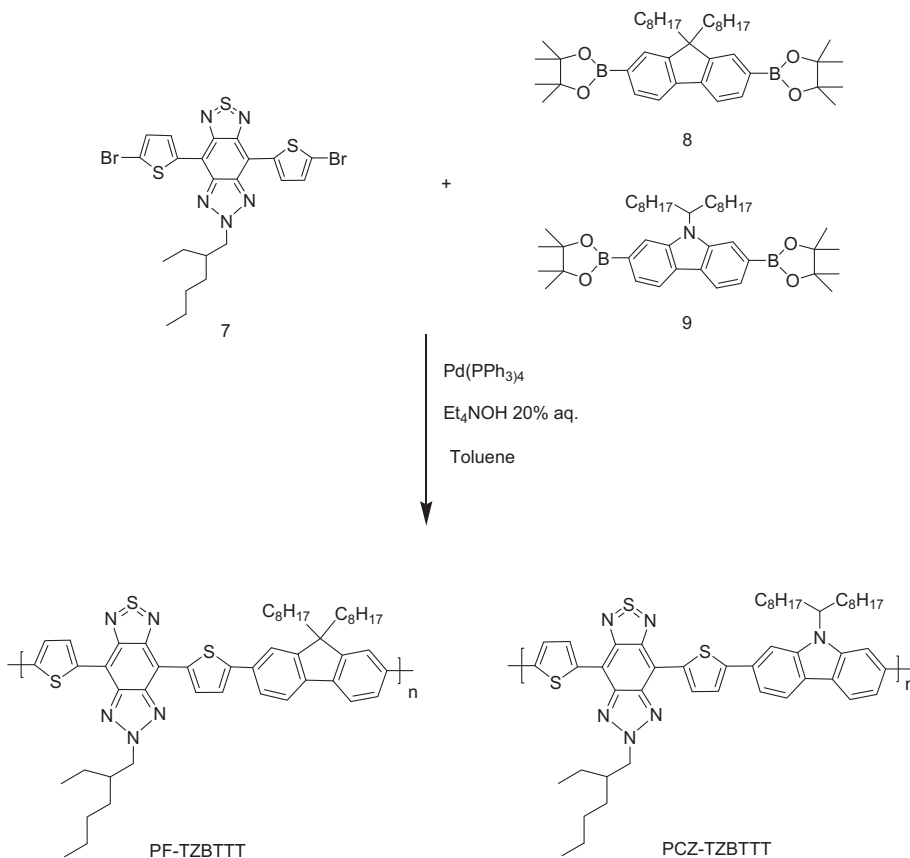
3. Results and discussion

3.1. Synthesis and characterization

The synthetic routes of the monomers and copolymers are shown in Schemes 1 and 2, respectively. Monomers 4,7-dibromo-5,6-dinitro-benzo[1,2,5]thiadiazole (**2**), 5,6-dinitro-4,7-bis(thiophen-2-yl)-benzo[1,2,5]thiadiazole (**3**), 5,6-diamino-4,7-bis(thiophen-2-yl)-benzo[1,2,5]thiadiazole (**4**), 2,7-bis(4',4',5',5'-tetramethyl-1',3',2'-dioxaborolan-2'-yl)-9,9-dioctylfluorene (**8**) and 2,7-bis(4',4',5',5'-tetramethyl-1',3',2'-dioxaborolan-2'-yl)-*N*-9'-heptadecanylethylcarbazole (**9**) were prepared according to the published literatures [21,26,39]. 4,8-Bis(thiophen-2-yl)-5*H*-[1,2,5]thiadiazolo[3,4-f]benzotriazole (**5**) was obtained by the reaction of monomer **4**, NaNO_2 and acetic acid. 4,8-Bis(thiophen-2-yl)-6-(2-ethylhexyl)-[1,2,5]thiadiazolo[3,4-f]benzotriazole (**6**) was synthesized from monomer **5** by adding potassium *t*-butoxide and 2-bromoethylheptane in dry DMF and



Scheme 1. Synthesis of the monomers.



Scheme 2. Synthesis of the copolymers.

heated to reflux in a low yield because of the existence of isomers. The key monomer 4,8-bis(5-bromo-thiophen-2-yl)-6-(2-ethylhexyl)-[1,2,5]thiadiazolo[3,4-f]-benzotriazole (**7**) was obtained by bromination of monomer **6** with NBS in THF.

The D–A type copolymers PF-TZBTTT and PCZ-TZBTTT were synthesized by Suzuki polycondensation of monomer **7** with monomer **8** or **9**, respectively. Pd(PPh₃)₄ was used as the catalyst in the polymerization. PF-TZBTTT and PCZ-TZBTTT have excellent solubility in common organic solvents such as chlorobenzene and *o*-DCB. The M_n of the two copolymers is 10.3 and 12.8 kDa, respectively, with the corresponding PDI of 2.90 and 2.92, respectively. The thermal properties of the copolymers were investigated by using TGA. As shown in Fig. 1 and Table 1, both of the copolymers have good thermal stability with 5% weight-loss temperature (T_d) of 418.2 and 401.0 °C for PF-TZBTTT and PCZ-TZBTTT, respectively.

3.2. Optical and electrochemical properties

The photo physical properties of the copolymers were investigated both in *o*-DCB solution and in thin films, which are shown in Fig. 2 and Table 2. PF-TZBTTT and PCZ-TZBTTT show similar absorption coefficients in the range of $10^{-3}/\text{cm}^{-1}$ and similar absorption spectra, which are common features of D–A copolymers. The absorption peaks at short wavelength (400–530 nm) originate from π to π^* transition of the polymers' conjugated backbone, while the absorption peaks at long wavelength (600–870 nm) could be attributed to the strong ICT interaction between the fluorene/carbazole donors and the TZBTTT acceptors [18]. It is found that the copolymers based on TZBTTT exhibit an obvious red-shifted ICT absorbance peak compared to those

previously reported D–A copolymers based on thiophene-substituted BT, such as poly[N-9'-heptadecanyl-2,7-carbazole-*alt*-5,5-(4',7'-di-2-thienyl-2',1',3'-benzothiadiazole)] (PCDTBT) and poly[2,7-(9-(2'-ethylhexyl)-9-hexyl-fluorene)-*alt*-5,5-(4',7'-di-2-thienyl-2',1',3'-benzothiadiazole)] (PFDTBT) [21,26]. The PCZ-TZBTTT has a maximum absorption peak at around 750 nm in solution, while it was reported that the absorption peak of PCDTBT

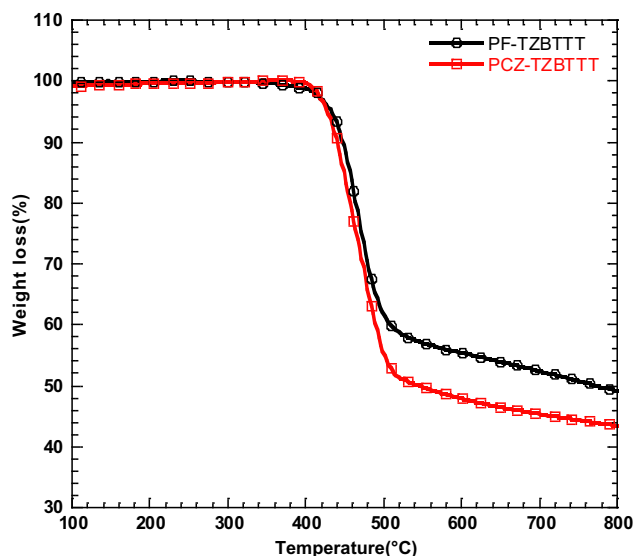


Fig. 1. TG plots of PF-TZBTTT and PCZ-TZBTTT.

Table 1
Molecular weight and thermal properties of the copolymers.

copolymers	M_n (kDa)	M_w (kDa)	PDI	T_d (°C)
PF-TZBTTT	10.3	29.9	2.90	418.2
PCZ-TZBTTT	12.8	37.4	2.92	401.0

is around 600 nm in the solution [21]. Similarly, the PF-TZBTTT also shows much stronger ICT characteristic compared with PFDTBT, of which the maximum absorption peaked at around 550 nm in the solution. The comparison above clearly illustrates that the TZBTTT-based D–A copolymers' band gaps can be effectively lowered due to the linkage of two electron-withdrawing groups, e.g. 1,2,5-thiadiazole and 2-ethylhexyl-1,2,3-triazole on the benzene ring. Moreover, it should be pointed out that the TZBTTT is a relatively weaker electron acceptor compared with previously reported benzo[1,2-*c*;4,5-*c'*]bis[1,2,5]thiadiazole or [1,2,5]thiadiazolo[3,4-*g*]quinoxaline, which have been proven to be too strong electron

Table 2
Electrochemical and optical properties of the polymers.

copolymer	λ_{abs} (nm) solution	λ_{abs} (nm) film	$E_{\text{g}}^{\text{opt}}$ (eV)	E_{ox} (eV)	E_{HOMO} (eV)	E_{LUMO} (eV)
PF-TZBTTT	425,756	440,798	1.33	0.76	−5.16	−3.83
PCZ-TZBTTT	420,754	438,785	1.35	0.78	−5.18	−3.83

withdraw acceptor units for PSCs and may affect the charge separation efficiencies between the resulting donor polymers and PC₆₁BM or PC₇₁BM. The maximum absorption of [1,2,5]thiadiazolo[3,4-*g*]quinoxaline-based D–A copolymers in chloroform located in about 810 nm [39] and it can be easily estimated that benzo[1,2-*c*;4,5-*c'*]bis[1,2,5]thiadiazole-based copolymer would have even narrower band gap because of the stronger electron-withdrawing ability than [1,2,5]thiadiazolo[3,4-*g*]quinoxaline. Both of the absorption spectra of TZBTTT-based copolymers show 30–40 nm red-shifted absorbance in the solid state compared with their corresponding ones in solution, indicating the presence of strong intermolecular interactions in the solid state. As shown in Table 2, the optical band gaps ($E_{\text{g}}^{\text{opt}}$) of the copolymers calculated from the absorption onset in the films are 1.33 eV for PF-TZBTTT and 1.35 eV for PCZ-TZBTTT, respectively.

The electrochemical behaviors of the copolymers were investigated by CV. The CV was performed in a solution of tetrabutylammonium hexafluorophosphate (Bu₄NPF₆) (0.1 M) in acetonitrile, using saturated calomel electrode (SCE) and a platinum wire as reference and counter electrode, respectively, at a scan rate of 50 mV/s at room temperature. A platinum electrode coated with thin copolymer film was used as the working electrode. The HOMO level values of the copolymers were calculated according to the following empirical formulas:

$$E_{\text{HOMO}} = -e(E_{\text{ox}} + 4.40) \text{ (eV)} \quad [46]$$

The E_{ox} is the onset oxidation and reduction potential vs SCE. The HOMO level values of these two copolymers were calculated to be −5.16 and −5.18 eV, respectively (Fig. 3). Both of the polymers' band gaps are narrower than those of previously reported BT-based

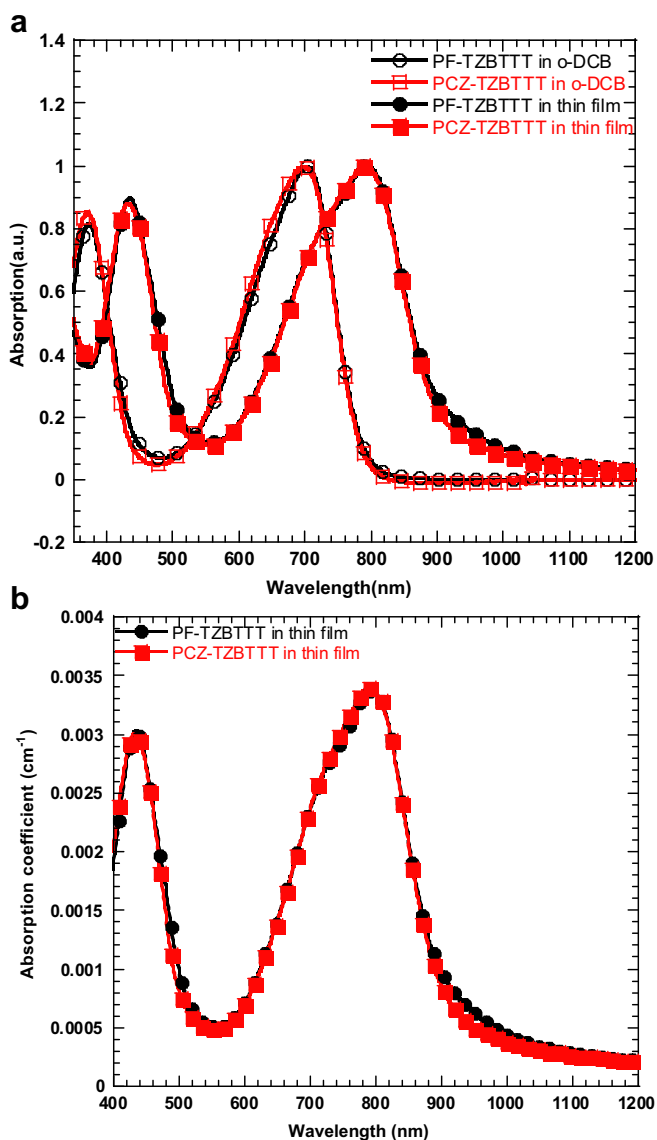


Fig. 2. (a) Normalized UV–vis absorption spectra of PF-TZBTTT and PCZ-TZBTTT in o-DCB solution and in thin films. (b) UV–visible absorption spectra of PF-TZBTTT and PCZ-TZBTTT in thin films.

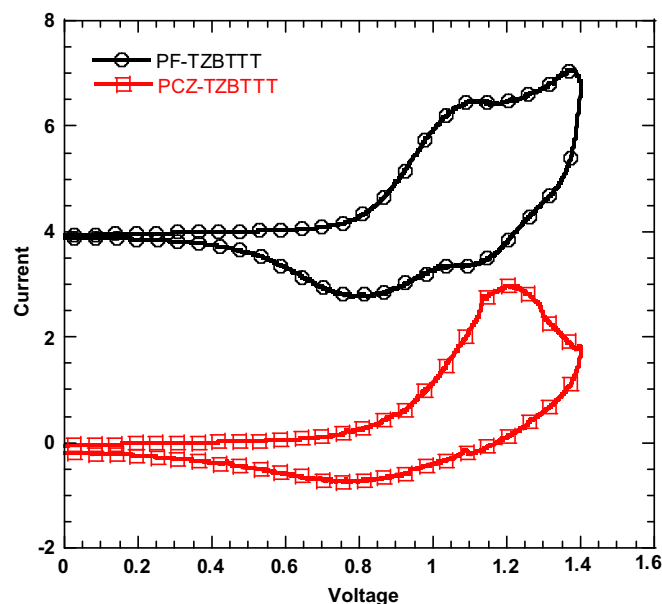


Fig. 3. Cyclic voltammograms of PF-TZBTTT and PCZ-TZBTTT.

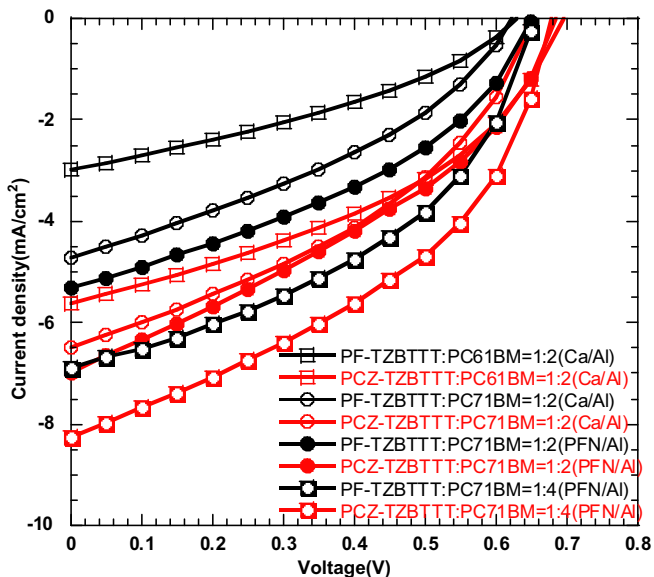


Fig. 4. J - V characteristics of the devices with the structure of ITO/PEDOT:PSS/copolymer:PC₆₁BM (PC₇₁BM)/Ca (PFN)/Al under the illumination of AM 1.5 G from a solar simulator (77 mW cm⁻²).

polyfluorene or polycarbazole copolymers, but are wider than those of [1,2,5]thiadiazolo[3,4-*g*]quinoxaline-based and benzo[1,2-*c*:4,5-*c'*]bis[1,2,5]thiadiazole-based ones. The lowest unoccupied molecular orbital (LUMO) level values of the copolymers were estimated from the HOMO energy levels and optical band gap (E_g^{opt}) using the equation

$$E_{\text{LUMO}} = E_{\text{HOMO}} + E_g^{\text{opt}}$$

As shown in Table 2, both of the LUMO levels of PF-TZBTTT and PCZ-TZBTTT are -3.83 eV. It has been reported that the E_g^{opt} , LUMO level and HOMO level of ideal donor polymer is 1.5, -3.9 and -5.4 eV, respectively [47]. Thus, both of the LUMO levels of the copolymers are close to the ideal donor polymer, whereas the E_g^{opt} of the copolymers is 0.24 and 0.22 eV narrower than the ideal E_g^{opt} , respectively, due to the high-lying HOMO levels.

3.3. Photovoltaic properties

Photovoltaic properties of the copolymers blended with PC₆₁BM or PC₇₁BM were investigated in PSC devices with two device configurations: ITO/PEDOT:PSS/copolymer:PC₆₁BM (or PC₇₁BM)/Ca/Al and ITO/PEDOT:PSS/copolymer:PC₆₁BM (or PC₇₁BM)/PFN/Al, where PFN was a water/alcohol soluble conjugated polymer material, and it was spin-coated onto the active layer to form the electron transporting cathode interlayer [48,49]. The PSC devices were fabricated with well-established procedures [18] and the active layers were spin-coated from *o*-DCB solution. The devices were tested under AM 1.5 G illumination (77 mW cm⁻²). Fig. 4 shows the current density-voltage characteristics of BHJ PSCs with two copolymers as the donors and PC₆₁BM (or PC₇₁BM) as the acceptors. Table 3 summarizes the performances of the devices. It can be seen that PCZ-TZBTTT showed better photovoltaic performances compared with PF-TZBTTT. The PCE of PCZ-TZBTTT/PC₆₁BM based device reached 1.94% with the J_{sc} , V_{oc} , and FF of 6.70 mA/cm², 0.7 V and 40%, respectively. As both of the copolymers showed little absorption in the range of 480–640 nm, PC₆₁BM was replaced to PC₇₁BM as the acceptor material to compensate the absorption of the active layer in this area. Consequently, the PCE was increased by

Table 3

Photovoltaic performance of the polymers measured under the illumination of simulated AM 1.5 G conditions (77 mW cm⁻²).

Copolymer	Blend ratio	Cathode	J_{sc} (mA/cm ²)	V_{oc} (V)	FF	PCE (%)
PF-TZBTTT	1:2 ^a	Ca/Al	2.98	0.65	0.34	0.85
	1:2 ^b	Ca/Al	4.73	0.60	0.37	1.36
	1:2 ^b	PFN/Al	5.30	0.65	0.39	1.74
	1:4 ^b	PFN/Al	6.90	0.65	0.44	2.56
PCZ-TZBTTT	1:2 ^a	Ca/Al	5.62	0.70	0.38	1.94
	1:2 ^b	Ca/Al	6.48	0.65	0.39	2.13
	1:2 ^b	PFN/Al	6.81	0.70	0.39	2.41
	1:4 ^b	PFN/Al	8.50	0.70	0.41	3.17

^a Blend with PC₆₁BM.

^b Blend with PC₇₁BM.

58% for PF-TZBTTT/PC₇₁BM based device and 15% for PCZ-TZBTTT/PC₇₁BM based device, compared to those of polymer/PC₆₁BM based devices. As an effective interfacial modification material, PFN has the potential for improving the PCE by enhancing the electron collection and decreasing the possibility of hole-electron recombination in the active layer [50,51]. Therefore, when Ca/Al was replaced with PFN/Al as the cathode, the performances of the resulting PSC devices was further increased. Besides, when the blend ratio of polymer:PC₇₁BM was changed from 1:2 to 1:4, the J_{sc} was further improved by 30% for both PF-TZBTTT and PCZ-TZBTTT based devices. Hence, it was found that the optimized PSCs devices based on PCZ-TZBTTT and PF-TZBTTT exhibited maximum PCEs of 3.17% and 2.56%, respectively. The external quantum efficiency (EQE) of the device based on the six blends illuminated by the monochromatic light was determined and shown in Fig. 5. All the devices showed broad photoresponse in the range from 400 nm to 900 nm. It was found that there is an obvious absorption improvement in the range of 530–600 nm as the ratio of PC₇₁BM increased, which is in accordance with the performance improvement of the resulting devices. Compared with the other devices, the PCZ-TZBTTT:PC₇₁BM (1:4) based device showed higher EQE (over 40%) in the range of 400–500 nm when using PFN/Al as the cathode. The hole mobilities of the donor conjugated polymers play a key role in the performance of BHJ-type PSCs. The hole mobilities

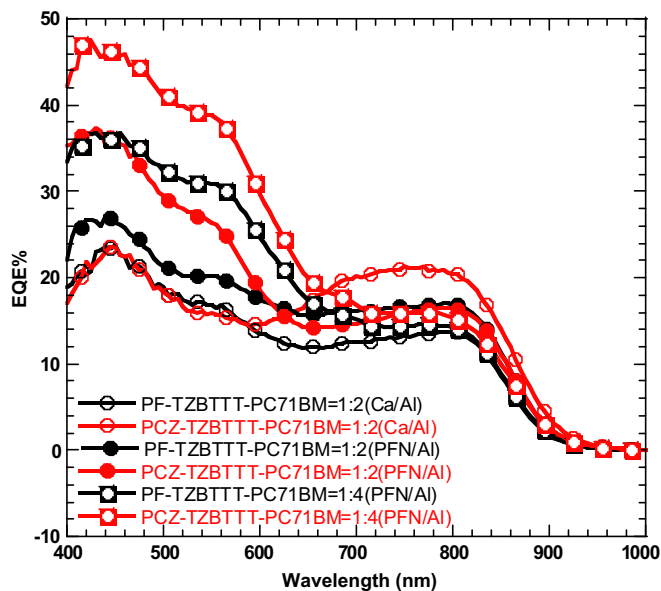


Fig. 5. EQE curves of the photovoltaic cells with polymer: PC₇₁BM = 1:2 (or 1:4) using Ca/Al (or PFN/Al) bilayer cathode as active layer, respectively.

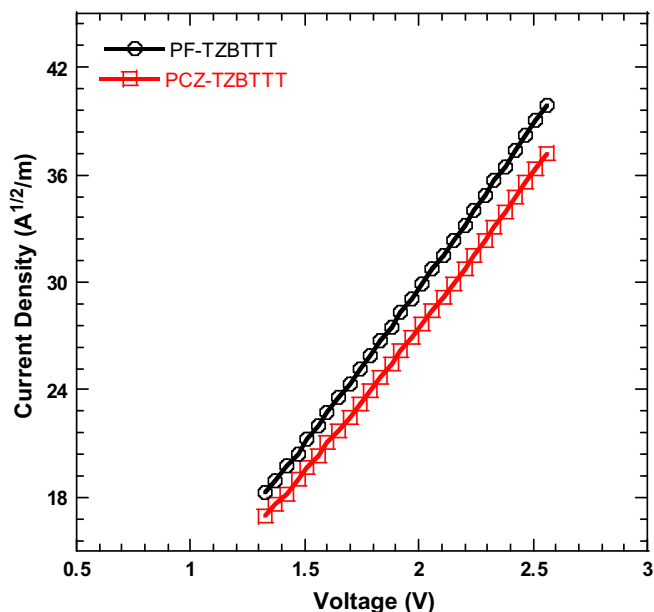


Fig. 6. Typical J vs V plots of the copolymers for the measurement of hole mobility by the SCLC method.

of the copolymers blended with PC₇₁BM were measured by using the SCLC method, where the current–density–voltage characteristics can be described by the equation $J_{\text{SCLC}} = (9/8)\epsilon_0\epsilon_r\mu_0(V^2/L^3)$ [52], where J is the current, μ_0 is the zero-field mobility, ϵ_0 is the permittivity of free space, ϵ_r is the relative permittivity of the material, L is the thickness of the active layer, and V is the effective voltage. Fig. 6 shows the $J^{1/2}$ – V characteristics of the blend of copolymers and PC₇₁BM obtained in the dark for hole-only devices with the configuration: ITO/PEDOT/active layer (75 nm)/MoO₃ (10 nm)/Al (90 nm). The perfect linear fitting in the figure indicates the $J^{1/2}$ – V characteristic follows the Mott–Gurney square law. The mobilities are $8.4 \times 10^{-5} \text{ cm}^2 \text{ V}^{-1} \text{ S}^{-1}$ for PF-TZBTTT:PC₇₁BM (1:4) blend and $8.1 \times 10^{-5} \text{ cm}^2 \text{ V}^{-1} \text{ S}^{-1}$ for PCZ-TZBTTT:PC₇₁BM (1:4) blend, respectively. Since both of the polymers have similar mobilities and absorption extinction coefficients, the difference in PSC performance observed between them may originate from different phase separations of their corresponding active layers. The mobilities of the blends are not high enough, which may be one of the reasons for the low FF of the resulting devices. It is known that the PSC active layers' mobilities depend on many factors, such as the substituted side chains on the polymers and the phase separation of the polymer/PCBM blends. The optimization of these factors is in progress, which may lead the improvement of these polymers' photovoltaic performance in near future.

4. Conclusions

In summary, two novel [1,2,5]thiadiazolo[3,4-*f*]benzotriazole-based copolymers, PF-TZBTTT and PCZ-TZBTTT have been successfully synthesized. The band gaps of the resulting copolymers were effectively narrowed to ~ 1.3 eV compared to previously reported BT based analogous polymers because of the induced extra electron deficient triazole groups on the benzene ring. Moreover their solubilities were also improved due to the linked alkyl side chains on the triazole rings. The photovoltaic properties of the resulting polymers were systematically studied and it was found that the resulting devices exhibited much improved device performance when using PC₇₁BM as the acceptors and a water/alcohol soluble

conjugated polymer PFN as the cathode modification layer. All the resulting devices exhibited a broad photo response range covering 400–900 nm. Among them, the PCE of PCZ-TZBTTT based devices reached 3.17% with a V_{oc} of 0.70 V, a J_{sc} of 8.50 mA cm^{-2} , and an FF of 0.41. All of these results indicate that [1,2,5]thiadiazolo[3,4-*f*]benzotriazole-based copolymers are promising candidates for application in photovoltaic devices.

Acknowledgments

The work was financially supported by the Natural Science Foundation of China (No. 21125419, 50990065, 51010003, 51073058, and 20904011), the Ministry of Science and Technology, China (MOST) National Research Project (no. 2009CB623601).

References

- [1] Yu G, Gao J, Hummelen JC, Wudl F, Heeger AJ. *Science* 1995;270(5243):1789–91.
- [2] Cheng Y-J, Yang S-H, Hsu C-S. *Chem Rev* 2009;109(11):5868–923.
- [3] Coakley KM, McGehee MD. *Chem Mater* 2004;23:4533–42.
- [4] Brabec CJ, Cravino A, Meissner D, Sariciftci NS, Fromherz T, Rispeens MT, et al. *Adv Funct Mater* 2001;11(5):374–80.
- [5] Günes S, Neugebauer H, Sariciftci NS. *Chem Rev* 2007;107(4):1324–38.
- [6] Peet J, Heeger AJ, Bazan GC. *Acc Chem Res* 2009;42(11):1700–8.
- [7] Service RF. *Science* 2011;332(6027):293.
- [8] van Mullekom HAM, Vekemans J, Havinga EE, Meijer EW. *Mater Sci Eng R* 2001;32(1):1–40.
- [9] Chen JW, Cao Y. *Acc Chem Res* 2009;42(11):1709–18.
- [10] Zhan XW, Zhu DB. *Polym Chem* 2011;1(4):409–19.
- [11] Huo L, Hou J, Zhang S, Chen H-Y, Yang Y. *Angew Chem Int Ed* 2010;49(8):1500–3.
- [12] Zhou QM, Hou Q, Zheng LP, Deng XY, Yu G, Cao Y. *Appl Phys Lett* 2004;84(10):1653–5.
- [13] Huo LJ, Guo X, Li YF, Hou JH. *Chem Commun* 2011;47(31):8850–2.
- [14] Shi QQ, Fan HJ, Liu Y, Hu W, Li YF, Zhan XW. *J Phys Chem C* 2010;114(39):16843–8.
- [15] Huang F, Chen K-S, Yip H-L, Hau SK, Acton O, Zhang Y, et al. *J Am Chem Soc* 2009;131(39):13886–7.
- [16] Zou YP, Najari A, Berrouard P, Beaupre S, Aich BR, Tao Y, et al. *J Am Chem Soc* 2010;132(15):5330–1.
- [17] Hou JH, Chen H-Y, Zhang S, Li G, Yang Y. *J Am Chem Soc* 2008;130(48):16144–5.
- [18] Zhang J, Cai WZ, Huang F, Wang EG, Zhong CM, Liu SJ, et al. *Macromolecules* 2011;44(4):894–901.
- [19] Wang M, Hu XW, Liu P, Li W, Gong X, Huang F, et al. *J Am Chem Soc* 2011;133(25):9638–41.
- [20] Zhao W, Cai WZ, Xu RX, Yang W, Gong X, Wu HB, et al. *Polymer* 2010;51(14):3196–202.
- [21] Blouin N, Michaud A, Leclerc M. *Adv Mater* 2007;19(17):2295–300.
- [22] Zhang Z-G, Min J, Zhang SY, Zhang J, Zhang MJ, Li YF. *Chem Commun* 2011;47(33):9474–6.
- [23] Wang EG, Hou LT, Wang ZQ, Hellstrom S, Zhang FL, Inganäs O, et al. *Adv Mater* 2010;22(46):5240–4.
- [24] Wang EG, Wang L, Lan LF, Luo C, Zhuang WL, Peng JB, et al. *Appl Phys Lett* 2008;92(3):033307-3.
- [25] Akhtaruzzaman M, Tomura M, Nishida J-I, Yamashita Y. *J Org Chem* 2004;69(9):2953–8.
- [26] Svensson M, Zhang FL, Veenstra SC, Verhees WJH, Hummelen JC, Kroon JM, et al. *Adv Mater* 2003;15(12):988–91.
- [27] Qin R, Li W, Li C, Du C, Veit C, Schleiermacher H-F, et al. *J Am Chem Soc* 2009;131(41):14612–3.
- [28] Du C, Li C, Li W, Chen X, Bo Z, Veit C, et al. *Macromolecules* 2011;44(19):7617–24.
- [29] Song J, Du C, Li C, Bo Z. *J Polym Sci Part A Polym Chem* 2011;49(19):4267–74.
- [30] Zhou H, Yang L, Stuart AC, Price SC, Liu S, You W. *Angew Chem Int Ed* 2011;50(13):2995–8.
- [31] Kitamura C, Tanaka S, Yamashita Y. *Chem Mater* 1996;8(2):570–8.
- [32] Steckler TT, Zhang X, Hwang J, Honeyager R, Ohira S, Zhang X-H, et al. *J Am Chem Soc* 2009;131(8):2824–6.
- [33] Li X, Liu A, Xun S, Qiao W, Wan X, Wang Z. *Org Lett* 2008;10(17):3785–7.
- [34] Yamashita Y, Ono K, Tomura M, Tanaka S. *Tetrahedron* 1997;53(29):10169–78.
- [35] Qian G, Dai B, Luo M, Yu D, Zhan J, Zhang Z, et al. *Chem Mater* 2008;20(19):6208–16.
- [36] Yu C-Y, Chen C-P, Chan S-H, Hwang G-W, Ting C. *Chem Mater* 2009;21(14):3262–9.
- [37] Bundgaard E, Krebs FC. *Macromolecules* 2006;39(8):2823–31.
- [38] Qian G, Zhong Z, Luo M, Yu D, Zhang Z, Ma D, et al. *J Phys Chem C* 2009;113(4):1589–95.

- [39] Perzon E, Wang XJ, Admassie S, Inganäs O, Andersson MR. *Polymer* 2006; 47(12):4261–8.
- [40] Perzon E, Zhang F, Andersson LM, Mammo W, Inganäs O, Andersson MR. *Adv Mater* 2007;19(20):3308–11.
- [41] Tanimoto A, Yamamoto T. *Macromolecules* 2006;39(10):3546–52.
- [42] Baran D, Balan A, Celebi S, Meana EB, Neugebauer H, Sariciftci NS, et al. *Chem Mater* 2010;22(9):2978–87.
- [43] Zhang LJ, He C, Chen J, Yuan P, Huang L, Zhang C, et al. *Macromolecules* 2010; 43(23):9771–8.
- [44] Price SC, Stuart AC, Yang L, Zhou H, You W. *J Am Chem Soc* 2011;133(12): 4625–31.
- [45] Tam TL, Li HR, Lam YM, Mhaisalkar SG, Grimsdale AC. *Org Lett* 2011;13(17): 4612–5.
- [46] Li YF, Cao Y, Gao J, Wang D, Yu G, Heeger AJ. *Synth Met* 1999;99(3):243–8.
- [47] Thompson BC, Fréchet JM. *Angew Chem Int Ed* 2008;47(1):58–77.
- [48] Huang F, Wu HB, Wang DL, Yang W, Cao Y. *Chem Mater* 2004;16(4): 708–16.
- [49] Huang F, Wu HB, Cao Y. *Chem Soc Rev* 2010;39(7):2500–21.
- [50] Luo J, Wu HB, He C, Li AY, Yang W, Cao Y. *Appl Phys Lett* 2009;95(4):043301-1.
- [51] He ZC, Zhang C, Xu XF, Zhang LJ, Huang L, Chen JW, et al. *Adv Mater* 2011; 23(27):3086–9.
- [52] Malliaras GG, Salem JR, Brock PJ, Scott C. *Phys Rev B* 1998;58(20):13411–4.